Copolymerization between A_3 and B_2 with Ring Formation and Different Intrinsic Reactivity in One of the Monomers

S. Pereda, A. Brandolin, E. M. Vallés, and C. Sarmoria*

Planta Piloto de Ingeniería Química (PLAPIQUI), UNS−CONICET, Camino La Carrindanga km 7, 8000 Bahía Blanca, Argentina

Received August 16, 2000; Revised Manuscript Received March 16, 2001

ABSTRACT: We present two models for the stepwise copolymerization between a three-functional monomer A_3 and a bifunctional monomer B_2 where both intramolecular reaction and different intrinsic reactivities of reactive sites are present. The difference in reactivities may be either on the A sites or the B sites, leading to two different models. The models may calculate both pregel and postgel parameters. One of the two models presents a nonsymmetrical response to the rate constant ratio. Each of the nonidealities was previously known to lead to a delay in gel point when considered individually; we find in this work that when present simultaneously they may either reinforce or compensate each other, depending on the reacting conditions. We reinterpret some experimental data from the literature using one of the models, with satisfactory results.

Introduction

Classical theories of polymerization consider ideal reaction, defined as one that verifies three assumptions: (a) all sites are equally reactive, (b) there is no substitution effect, and (c) there is no intramolecular reaction. These ideal reactions have been modeled by many authors.[1−7] In many real systems, one or more of those three assumptions are not valid. When more realistic models have been attempted, in general only one of the ideal assumptions has been dropped at one time.

First shell substitution effect in an otherwise ideal reaction has been treated both for homopolymerizations and copolymerizations.[8−12] Systems with neither an intramolecular reaction nor a substitution effect but where some sites are intrinsically more reactive than others have also been modeled.[4,7,13,14] The case where all sites are equally reactive, there is no substitution effect but intramolecular reaction is allowed has been modeled with a variety of methods: purely kinetic,[15,16] Monte Carlo simulations,[17−20] Spanning Tree or cascade theory,[21,22] rate theory,[23−25] kinetic−Markovian models,[26−28] and other approaches.[29−32]

For some systems, it is more realistic to consider two simultaneous departures from the ideal assumptions than to consider only one. Published models have considered the simultaneous presence of cyclization and substitution effects. The earliest ones were developed by Gordon and co-workers,[33,34] who used the Spanning Tree approach. Kasehagen et al.[35] and Fahey et al.[36] have recently presented models that include those two nonidealities but employ other mathematical approaches.

To our knowledge, no models have been published in the open literature that include simultaneous presence of intramolecular reaction and sites with different intrinsic reactivities. This is the situation we address in this paper. This new model gives us the opportunity to study whether the effects of each non ideality on the final material are additive or not. Both intramolecular reaction and difference in intrinsic reactivities of sites have been reported to produce delays in gel point when considered separately.[13,14,22,37−42] Both lead to lower weight-average molecular weights in the pregel region than would be expected from ideal theories. Although difference in intrinsic reactivities would not preclude the formation of a perfect network at complete reaction, intramolecular reaction would. Possible defects include the presence of a measurable sol fraction at complete reaction, and a reduction in the number of elastically active network chains.[17−22,24−27]

We model the stepwise, irreversible reaction of a trifunctional monomer symbolized as A_3 with a bifunctional monomer indicated as B_2. The only possible reaction is A−B, so the resulting copolymers are strictly alternating. We also assume that the reaction never becomes diffusionally controlled, as customary in this type of modeling work. We keep only one of the ideal reaction assumptions, namely that there is no substitution effect. We allow both intramolecular reaction and different reactivities of sites in one of the reactants. Intramolecular reaction becomes especially important in reactions carried out in dilute conditions.

In the models we present in this paper, we only allow the formation of the smallest possible ring. It is an approximation, but it provides a useful tool that allows us to study the relative importance of each nonideality on the problem at hand. This approximation is reasonable in view of previous work that has shown that for flexible polymers the smallest one is the single most abundant ring of those present in a polymerization system,[17−19,26,37] when all sites are equally reactive. They also contribute the most to the composition of the sol fraction that remains at complete reaction.[37] Even so, other works[19,22] have reported using rings of all sizes in order to model elastic data in polyurethane systems with equal reactivity on all sites. On the other hand, Dušek et al.[21] and Ilavský and Dušek[22] have argued that the definition of a ring is ambiguous in the gel, where there would naturally be circuits present that do not affect elasticity. A large ring contains reactive sites along its contour that allows it to be activated, that is, to become elastically effective.[21,22] This point of view lessens the requirement of accounting for all sizes of rings; taking into consideration a few of the smallest ones should give a good approximation.

The functionality of the monomer where there are sites of different reactivity may affect the behavior of the system. We explore here the two possible situations

* Corresponding author. Telephone: 54-91-4861700. Fax: 54-91-4861600. E-mail: csarmoria@plapiqui.edu.ar.

10.1021/ma001438m CCC: $20.00
Published on Web 05/24/2001

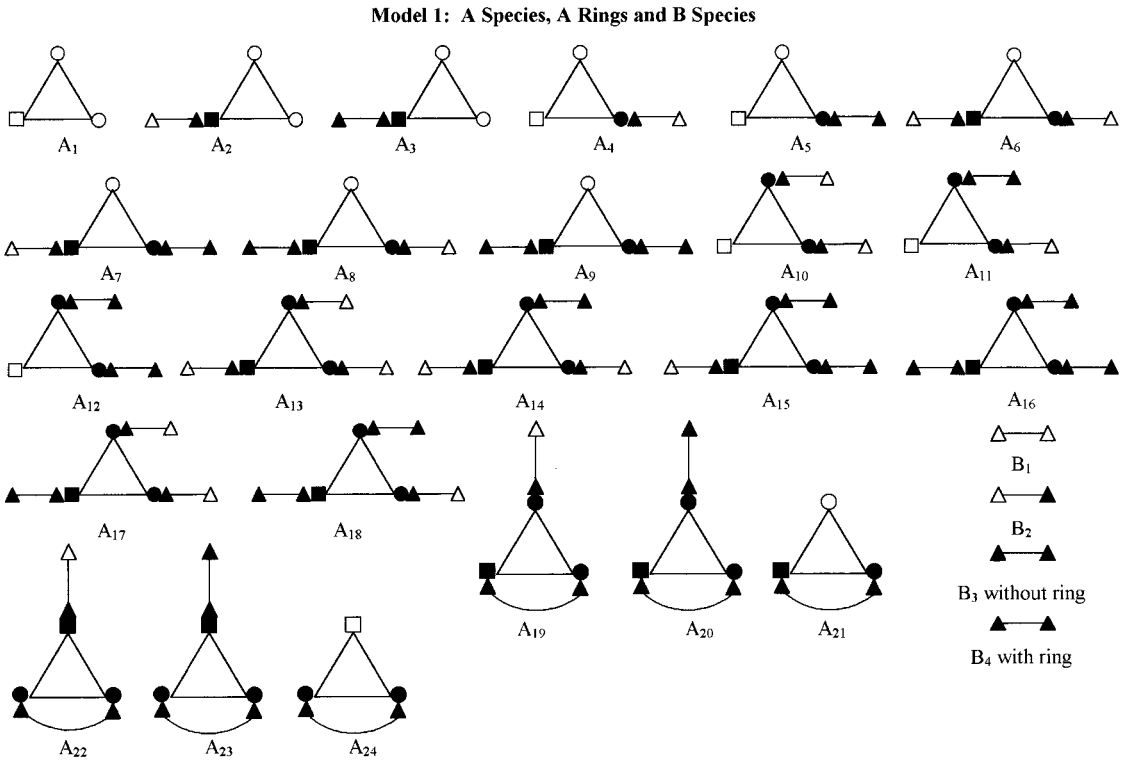

Figure 1. Structures necessary to describe model 1, with different reactivities on A sites. Circles and squares represent A sites with different intrinsic reactivities; triangles represent B sites. Open symbols correspond to unreacted sites; filled symbols to reacted functional groups.

in an $A_3 + B_2$ system, where A_3 is a monomer with three reactive A sites and B_2 is a monomer with two reactive B sites. In the first case, one of the sites on A_3 has a different reactivity, while both sites on B_2 are equally reactive. Polyesters synthesized from glycerol and aliphatic diols may present this behavior. In the second case, B_2 is the monomer that has two sites with different reactivities, while the three sites on A_3 are equally reactive. This situation would model the synthesis of polyurethanes from toluene diisocyanate and symmetric triols.

Our models predict weight-average molecular weights as a function of conversion, gel point, and post-gel parameters such as sol and gel fractions, fraction of elastically effective material and fraction of pendant material.

In what follows we show the details of one of the two models, discuss its predictions and compare them with experimental data from the literature. Results from the second model are also discussed in detail, but its governing equations are not shown since they are obtained following a procedure analogous to the one used in model 1.

First Model. $A_3 + B_2$ with Intramolecular Reaction and Different Reactivities in A Sites

We model this system using the kinetic−recursive or kinetic−Markovian approach.[6,7,27,28] In this approach, modeling is performed in two steps. The first one is a kinetic step, where conceptual "superspecies" must be defined in such a way as to be able to describe the entire system with them. Kinetic equations are set up to describe the way in which the concentrations of the "superspecies" change as conversion increases. The second step is a Markovian step, where all the superspecies combine at random to reproduce the structure of the polymer system.[28]

All the nonidealities of the system must be taken into account in the kinetic step, and because of this the superspecies must be large enough to accommodate those nonidealities. In the case under study in this section, the A monomer has two sites of the same intrinsic reactivity and a third site with a different reactivity. We will call them A^1 sites and A^2 site, respectively. The A^2 site may be either more reactive or less reactive than the other two. The B monomer has two sites with identical reactivities. There is no substitution effect, but intramolecular reaction is allowed. Only the smallest ring, the one that involves one B monomer and one A monomer, is allowed. This is an approximation, but one that considers the most numerous of the rings that may form, as others have verified in several Monte Carlo simulations.[17−19] The A monomer is considered to be relatively small, and the B monomer is assumed to be a chain long enough for Gaussian end-to-end distance distributions to be valid for it. For this situation, the 24 superspecies shown in Figure 1 are necessary. Notice that sites with different reactivities are indicated with different symbols and that the allowed rings are completely contained in the selected superspecies.

Superspecies may react with one another to give as a result a different superspecies. For example, species A_2 may react with any unreacted A^1 site or A^2 site to give species A_3 as indicated in eqs 1 and 2. Notice that two equations are necessary because of the different kinetic rates involved.

$$A_2 + A^1 \xrightarrow{k_1} A_3 \tag{1}$$

$$A_2 + A^2 \xrightarrow{k_2} A_3 \tag{2}$$

Here k_1 is the kinetic rate constant associated with the reaction of A^1 and B sites, and k_2 is the kinetic rate

constant associated with the reaction of A^2 and B sites. Other possible reactions for the A_2 structure include reaction with a B group. It may belong to an unreacted B monomer, designated from now on as B_1 (see Figure 1), or to a B monomer with one end already reacted. This is designated as B_2. Reaction of structure A_2 with B_2 gives A_7, reaction with B_1 gives A_6, and intramolecular reaction gives A_{21}.

Twenty four simultaneous kinetic differential equations are set up, one for each of the species used to describe the system. They are shown in the Appendix. In the terms that describe intramolecular reactions, the concentration of one chain end around the other appears with the symbol C_j. We employ eq 3 to estimate this value.

$$C_j = \frac{1}{D_G}\left(\frac{1.5}{jn_e\pi}\right)^{1.5}\frac{1}{N_A {l_B}^3}\ \text{mol/volume} \tag{3}$$

Equation 3 is the Gaussian expression for the concentration of one chain end around the other for a real chain with jn_e links of length l_B. In our case $j = 1$, since the only rings allowed contain only one B monomer chain. In this expression N_A is Avogadro's number, introduced there so that the units of the concentration will be mol/volume. For a perfectly flexible chain, the constant D_G is unity. This constant differs from unity when dealing with chains that are not perfectly flexible.[23,43,44] Instead of using the constant D_G, other authors have introduced a kinetic constant for intramolecular reaction different from the one used for intermolecular reaction.[15,34] Both approaches are equivalent.

The kinetic differential equations are integrated numerically using Gear's method. As a result of this integration, the concentrations of the 24 structures are obtained as functions of time ($A_i(t)$, $i = 1-24$, $B_j(t)$, $j = 1-4$).

Conversion (p_A) may be evaluated using the relationship in eq 4.

$$p_A = \frac{3A_1(0) - A^1(t) - A^2(t)}{3A_1(0)} \tag{4}$$

Since rings are being produced, some form of concentration must be evaluated in order to be able to quantify them. The chosen quantity is the relative ring concentration, which may be calculated as in eq 5.

$$[\text{rings}]_{rel} = \frac{\text{number of ring-closing A sites}}{\text{number of reacted A sites}} = \frac{\sum_{i=19}^{24} A_i(t)}{3A_1(0)p_A} \tag{5}$$

The next step is to reconstruct the macromolecules by randomly combining the 24 superspecies. It is not really necessary to reconstruct each of the infinitely many macromolecules present in the system. What we are interested in is the evaluation of average properties such as the weight-average molecular weight. This is what we show next.

Evaluation of the Weight-Average Molecular Weight (M_w). To evaluate this quantity, we randomly pick a monomer unit from the reacting system. The chosen monomer becomes a *root*. The probability of picking an A root or a B root is equal to the weight fraction of the respective unit in the system, as indicated in eqs 6 and 7.

$$P(\text{A root}) = w_A = \frac{M_A A_1(0)}{M_A A_1(0) + M_B B_1(0)} \tag{6}$$

$$P(\text{B root}) = w_B = 1 - w_A \tag{7}$$

Here M_A and M_B are the molecular weights of A monomer and B monomer. Making use of the concept of conditional expectation,[6,7,45] the general formula for the evaluation of the weight-average molecular weight is given by eq 8,

$$M_w = E(W|\text{A root})\,P(\text{A root}) + E(W|\text{B root})\,P(\text{B root}) = E(W|\text{A root})w_A + E(W|\text{B root})w_B \tag{8}$$

where $E(W|\text{A root})$ and $E(W|\text{B root})$ represent the expected weight given an A or B monomer is selected, respectively. These quantities are obtained as described in the Appendix.

Gel Point. At the gel point, M_w diverges. Past that conversion, the numerical method gives negative values for M_w. This fact could be used to calculate the gel point to any desired accuracy, by restarting the numerical integration at the last point where M_w was positive with smaller integration steps as many times as necessary to reach the prescribed accuracy. Since experimentally the gel point may be measured with errors of about 5%, a precision of ± 0.001 in the calculated critical conversion was more than adequate. This could generally be achieved in less than five iterations of the restarting procedure just described.

Weight Fraction of Soluble Material. To find this quantity, again a root is chosen at random. The probabilities associated with an A root or a B root are w_A and w_B. The chosen root will be part of the sol fraction if walking out of it in all directions, we eventually reach a finite end. This is expressed as

$$w_s = w_A\,P(F|\text{A root}) + w_B\,P(F|\text{B root}) \tag{9}$$

where $P(F|\text{A root})$ and $P(F|\text{B root})$ are the probabilities of having chosen a finite molecule given that the root was either an A or B monomer, respectively. For details on the calculation of both probabilities, see the Appendix.

Weight Fraction of Elastically Effective Material. Following a similar approach as that used for the sol fraction, we use conditioning to find

$$w_e = w_A\,P(\text{el.eff}|\text{A root}) + w_B\,P(\text{el.eff}|\text{B root}) \tag{10}$$

where $P(\text{el.eff}|\text{A root})$ and $P(\text{el.eff}|\text{B root})$ are the probabilities that a structure is part of the elastically effective material given either an A monomer or a B monomer was selected. The expressions for these probabilities are given in the Appendix.

The remaining parameters are calculated by definition as indicated in the following equations:

Weight Fraction of Pendant Material. By definition

$$w_p = 1 - w_S - w_e \tag{11}$$

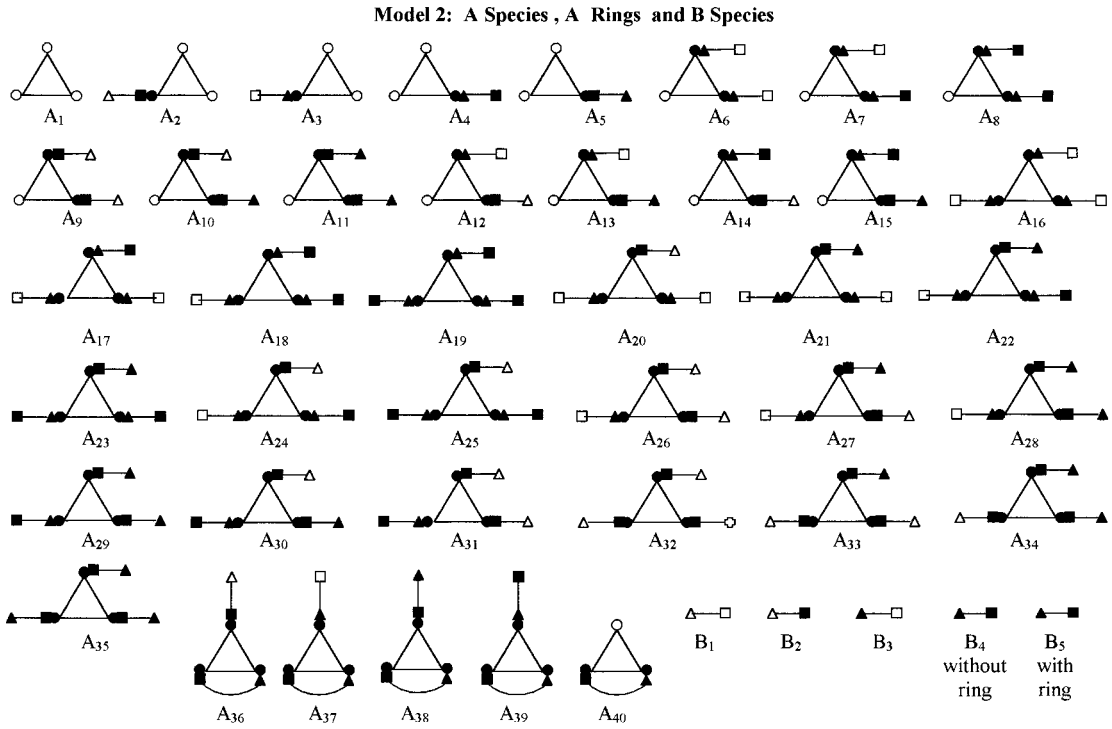

Figure 2. Structures necessary to describe model 2, with different reactivities on B sites. Squares and triangles represent B sites with different reactivities; circles represent A sites. Open symbols correspond to unreacted sites; filled symbols to reacted sites.

Concentration of Effective Junctions and Strands

$$\mu = (1 - P(F^{\text{out}}B_3))^3 A_{16}(t) \tag{12}$$

$$\nu = \frac{3}{2}\mu \tag{13}$$

where $P(F^{\text{out}}B_3)$ is the probability of finding a finite end when looking out of a B_3 unit. This quantity is calculated as indicated in the Appendix.

Entanglement Trapping Factor

$$Te = (1 - P(F^{\text{out}}B_3))^4 \tag{14}$$

Second Model. $A_3 + B_2$ with Intramolecular Reaction and Different Reactivity in B Sites

The model is developed following an approach similar to the one shown for the first model. In this case, 40 superspecies are needed, the ones shown in Figure 2. As in the first model, kinetic balance equations must be set up. Since there are 40 superspecies, a system of 40 simultaneous differential equations is necessary. Quantities such as weight-average molecular weight, sol and gel fraction, fraction of elastically effective material, concentration of elastically effective strands and junctions and entanglement trapping factor are calculated in a way analogous to the one presented for the first model. The equations are available from the authors upon request.

Results and Discussion

To test the model, several parameters were varied. The ones considered were the ratio of kinetic constants associated with sites A^1 and A^2 (k_1/k_2), the degree of dilution, the number of bonds, and the bond length. The base case considered was a reaction carried out without solvent, where the A monomer is very small and the B monomer is a perfectly flexible chain of 20 bonds. The bond length was assumed to be 1.5 Å.

As a first step, the model was tested under the ideal conditions: no rings allowed and $k_1/k_2 = 1$. The well-known ideal results were obtained: the gel point found numerically agreed to any desired accuracy with the formula

$$p_{\text{A,gel}} = \sqrt{\frac{1}{2r}} \tag{15}$$

where $p_{\text{A,gel}}$ is the conversion at the gel point, and r is the stoichiometric imbalance. The weight-average molecular weight in the pregel region agreed to any desired accuracy with the expression

$$M_w = \frac{\frac{2}{3}r(1 + r(p_A)^2)M_A{}^2 + 4rp_AM_AM_B + (1 + 2r(p_A)^2)M_B{}^2}{\left(\frac{2}{3}rM_A + M_B\right)(1 - 2r(p_A)^2)} \tag{16}$$

where M_A and M_B are the molecular weights of the monomers. The values of sol fraction, gel fraction, and fraction of pendant material also agreed with published expressions for the ideal copolymerization.[2,3,6,7] The models also reduced correctly to the already studied cases allowing just one nonideality at a time, that is, either rings are present or the ratio k_1/k_2 is not unity.

The response of the first model is not symmetric with respect to the k_1/k_2 ratio. For example, the results for $k_1/k_2 = 0.05$ are different from those obtained for $k_1/k_2 = 20$. This is not evident in the gel point results, but it is easily observed by comparing relative ring

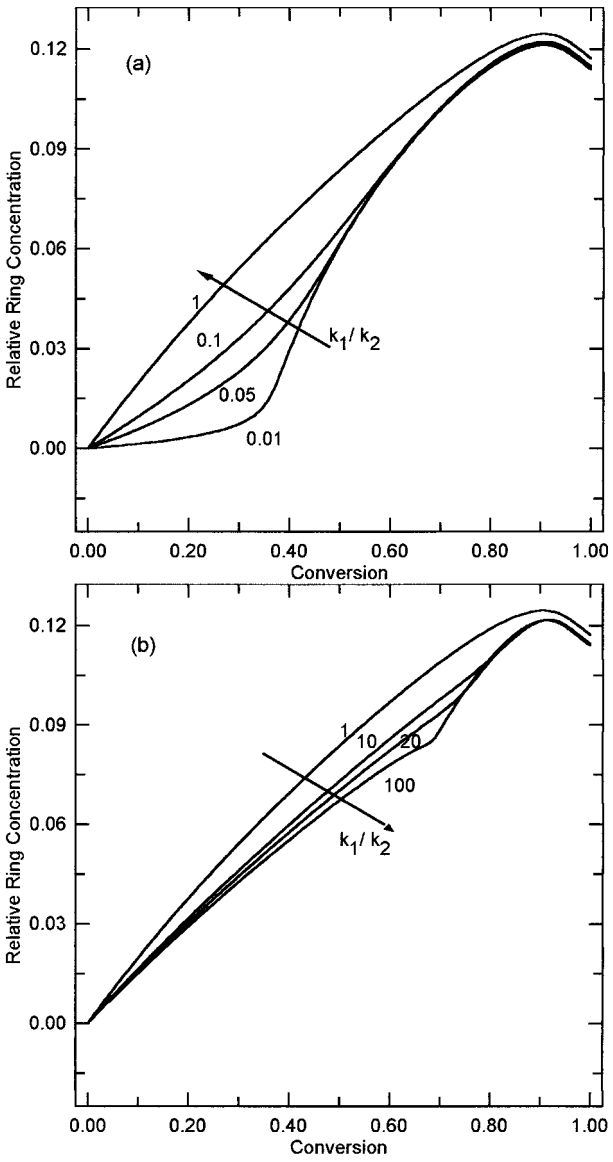

Figure 3. Relative ring concentration as a function of conversion for a system with different reactivity on A sites: (a) rate constant ratios lower than unity; (b) rate constant ratios larger than unity. The system contains no solvent.

concentrations calculated by means of eq 5. Figure 3 shows relative ring concentrations as functions of conversion for different k_1/k_2 ratios. Those corresponding to rate constant ratios lower than unity are in part a of the figure, and those higher than unity in part b. Please note that the chosen ratios in parts a and b of Figure 3 are multiplicative inverses of each other. The lack of symmetry of the response is evident. It may be observed that the highest level of ring formation is achieved for a rate constant ratio of unity; when reactivities are very different, ring formation is delayed. This may be explained because in such a case the less reactive sites tend not to react until the more reactive ones are almost completely consumed. Since half of the possible ring-containing structures (species A_{19}, A_{20}, and A_{21} in Figure 1) require the reaction of both an A^1 and an A^2 site, fewer rings can form at the early stages of the reaction. The tendency to delay ring formation for rate constant ratios other than unity is also observed for the case where the difference in reactivity is in the B sites. Since there are only two such sites, in that system the response is symmetric with respect to the k_1/k_2 ratio.

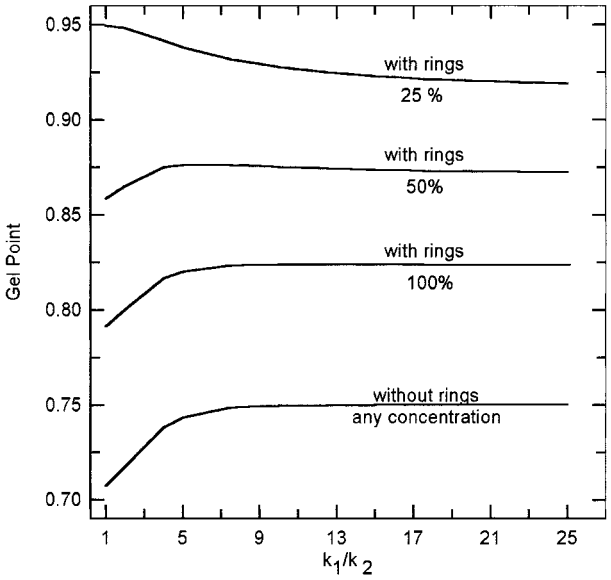

Figure 4. Calculated gel points for a model 2 system for different rate constant ratios and different concentrations of reactive species.

The $A_3 + B_2$ system gels at a conversion of 0.707 under ideal conditions for a stoichiometrically balanced system ($r = 1$). Both difference in rate constant ratios and presence of intramolecular reaction tend to delay the gel point when taken individually. When both nonidealities are present simultaneously, different behaviors are possible. We show in Figure 4 the calculated gel points for a system that corresponds to model 2 for different concentrations of reactive species (polymer and monomers) and different rate constant ratios. The solvent present in the lower concentration systems is inert toward the reaction. Curves are shown for a system without any rings allowed, and for systems with rings at different reactive species concentrations. Ring formation is favored by dilute reacting conditions, so lower concentrations translate into more important levels of ring formation. We may observe in the figure that ring formation is the single most important factor affecting the gel point. At any given concentration, change of rate constant ratio may change the gel point by at most 0.05, while the change in concentration (with rings present) may change it by up to 0.25. This is a general result both for model 1 and model 2 systems.

It may be observed that whenever the rate constant ratio is kept constant at any given value, a decrease in concentration leads to an increase in gel point delay. For example, for the particular case of $k_1/k_2 = 20$ in Figure 4, if no rings are allowed, gelation occurs at $p_A = 0.750$. The undiluted system with rings allowed gels at $p_A = 0.824$, and the gel point increases noticeably with dilution, as may be observed in Figure 4. This particular behavior is due to the presence of an intramolecular reaction, which is favored by dilute reaction conditions. Similar results are obtained for any model 2 system when the rate constant ratio is kept constant and the concentration of polymer is varied. However, if the concentration is fixed and the rate constant ratio increases, the gel point may either increase or decrease, depending on the concentration level. We see in Figure 4 that when no rings are allowed an increase in rate constant ratio always leads to an increase in gel point. The same is true for a completely undiluted system with rings. A system consisting of 25%

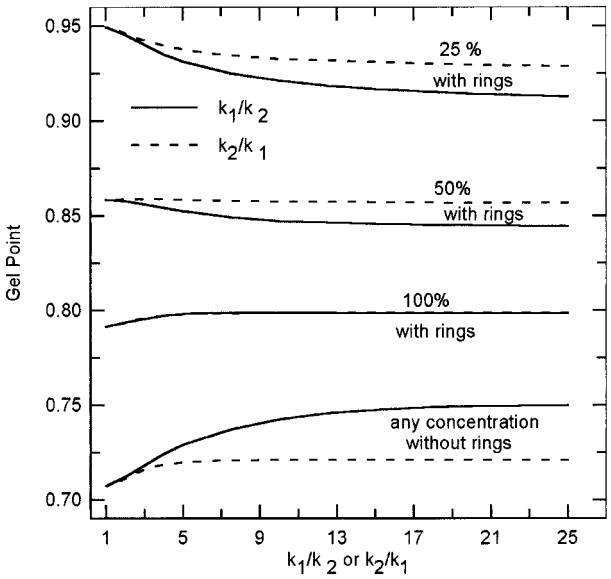

Figure 5. Calculated gel points for a model 1 system for different rate constant ratios and different concentrations of reactive species. Both k_1/k_2 and k_2/k_1 are represented on the abscissa.

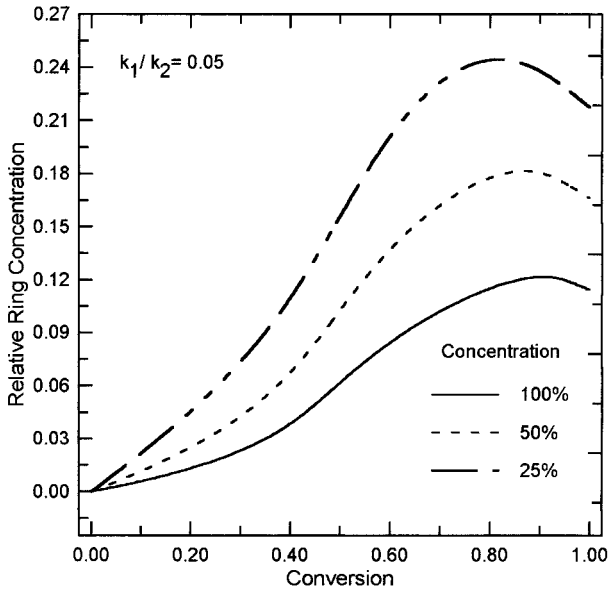

Figure 6. Relative ring concentration for a system with different reactivity on A sites, $k_1/k_2 = 0.05$ and different concentrations of reactive species.

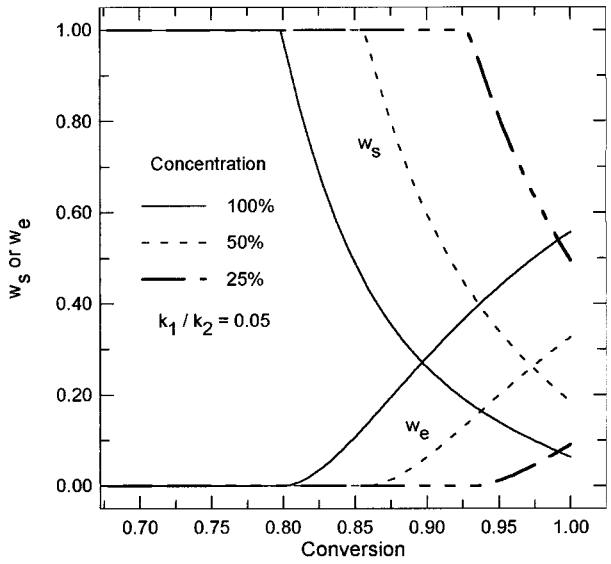

Figure 7. Weight fraction of soluble material and of elastically effective material for a system with different reactivity on A sites, $k_1/k_2 = 0.05$, and different concentrations of reactive species.

reactive species and 75% inert solvent, on the other hand, tends to decrease its gel point as the rate constant ratio increases. This means that at this particular concentration a more severely nonideal system tends to get closer to the ideal gel point result, something contrary to intuition. The two nonidealities are compensating their respective effects to a certain extent. This is possible since, as already discussed, ring formation tends to be delayed as the rate constant ratio deviates from unity. It is possible to slow ring formation long enough to minimize its impact on the gel point, as exemplified by the curve of 25% reactive species in Figure 4. A similar interplay of compensation effects is observed for systems corresponding to model 1, as shown in Figure 5. This system is unsymmetrical with respect to the rate constant ratio, so the abscissas of the figure include both k_1/k_2 and its inverse. It is interesting to note that at no dilution and with rings allowed, this system behaves symmetrically with respect to k_1/k_2. We may again observe that, also for model 1 systems, ring formation is capable of producing a much larger gel point delay than rate constant ratio can. As a confirmation that ring formation really increases as the system becomes more diluted, we show in Figure 6 the relative ring concentration as a function of conversion for a particular k_1/k_2 value and three different reactive species concentrations. Similar trends have been obtained for other values of k_1/k_2.

The postgel parameters also show a variation in their values due to the simultaneous presence of ring formation and difference in reactivity. Figure 7 shows a comparison of the weight fraction of soluble material (w_s) and weight fraction of elastically effective material (w_e) as functions of conversion at different dilutions for model 1 (different reactivity on A sites) when $k_1/k_2 = 0.05$. Every case results in imperfect networks at complete reaction, since ring formation is allowed. This translates into elastic fractions lower than unity and sol fractions greater than zero. Similar curves are obtained for other values of k_1/k_2 and for other reactive species concentrations. Systems that correspond to model 2 behave similarly. Note that those systems that gel later reach complete reaction with a more important level of flaws than those that gel earlier, closer to the ideal value of 0.707. The same interplay of compensating effects already discussed regarding the gel point affects the postgel properties.

To verify whether these models were capable of explaining actual experimental data, we analyzed data from the literature. Flory[39] reported on a series of experiments by Kienle et al.[46−48] on the reaction of glycerol with various dibasic acids. They reported gel points of 0.765 ± 0.01, higher than the ideally expected value of 0.707. Glycerol has two primary hydroxyl groups and one secondary hydroxyl group, this one being less reactive than the other two. However, consideration of this difference in reactivity was not enough to explain the discrepancy.[39] Intramolecular reaction appears as a logical explanation, but up to this date there has been no quantitative explanation of these results. We used our model 1 to try to simulate this problem.

Table 1. Experimental Data for Polyesters and Theoretical Predictions for Gel Points

diacid	mol wt	n_B	init. concn (mol/cm^3)	P_{gel}(no rings) ($k_1/k_2 = 10/3$)	P_{gel}(rings) ($k_1/k_2 = 10/3$)	D_G
succinic	118.1	8	8.08×10^{-3}	0.72	0.76	5.0
adipic	146.1	10	6.40×10^{-3}	0.72	0.76	4.5
sebacic	202.2	14	4.82×10^{-3}	0.72	0.76	3.5

The reactivity of primary alcohols relative to that of secondary alcohols is about 10:3.[49] Another necessary piece of information is the number of bonds in a closed cycle, n_B. The diacids reported in the cited works were phthalic acid, succinic acid, adipic acid and sebacic acid. Our model is adequate for treatment of all but phthalic acid, a reagent with a structure that is too stiff to accommodate the assumptions of our model. The monomer molecular weights, concentrations used, and number of bonds in a closed cycle are reported in Table 1. We also report the gel point calculated without rings, the gel point with rings, and the Gaussian factor (D_G) (see eq 3). The value D_G is largest for the smallest structure, and diminishes in value as the structures become larger. This is to be expected, since a factor of 1 corresponds to very long, flexible chains, and the chains in these reagents are short enough to present some stiffness. Larger D_G values are expected as the chains get shorter, just as shown here. We conclude that this model is adequate to interpret the data, and that in the reported esterifications there is ring formation.

Conclusions

Results indicate that both nonidealities affect the properties of the network significantly, increasing its imperfections. At fixed rate constant ratios, increasing dilution will always increase the gel point value and the final network flaws. At fixed concentrations, working at rate constant ratios farther away from unity may either increase or decrease the gel point value and the network flaws, depending on the concentration used. Some level of compensation between the two effects is possible.

The results suggest that the most important of the two nonidealities is the presence of intramolecular reaction. This is the nonideality that causes the largest departures from ideal behavior. Experimental data from the literature may be reinterpreted by use of this model.

Acknowledgment. This work was supported by CONICET and Universidad Nacional del Sur (UNS).

Appendix A

Kinetic Equations for $A_3 + B_2$ with Intramolecular Reaction and Different Reactivity in A Sites. Equations 17−40 are the kinetic balances for the 24 superspecies shown in Figure 1. In these equations A_i ($i = 1-24$), B_i ($i = 1-4$), A^1, and A^2 stand for species concentration.

$$\frac{dA_1(t)}{dt} = -2k_2B_1(t)A_1(t) - k_2B_2(t)A_1(t) - 4k_1B_1(t)A_1(t) - 2k_1B_2(t)A_1(t) \quad (17)$$

$$\frac{dA_2(t)}{dt} = 2k_2B_1(t)A_1(t) - k_1A^1(t)A_2(t) - k_2A^2(t)A_2(t) - 4k_1B_1(t)A_2(t) - 2k_1B_2(t)A_2(t) - 2k_1C_jA_2(t) \quad (18)$$

$$\frac{dA_3(t)}{dt} = k_2B_2(t)A_1(t) + k_1A^1(t)A_2(t) + k_2A^2(t)A_2(t) - 4k_1B_1(t)A_3(t) - 2k_1B_2(t)A_3(t) \quad (19)$$

$$\frac{dA_4(t)}{dt} = 4k_1B_1(t)A_1(t) - k_1A^1(t)A_4(t) - k_2A^2(t)A_4(t) - 2k_2B_1(t)A_4(t) - k_2B_2(t)A_4(t) - 2k_1B_1(t)A_4(t) - k_1B_2(t)A_4(t) - k_2C_jA_4(t) - k_1C_jA_4(t) \quad (20)$$

$$\frac{dA_5(t)}{dt} = 2k_1B_2(t)A_1(t) + k_1A^1(t)A_4(t) + k_2A^2(t)A_4(t) - 2k_2B_1(t)A_5(t) - k_2B_2(t)A_5(t) - 2k_1B_1(t)A_5(t) - k_1B_2(t)A_5(t) \quad (21)$$

$$\frac{dA_6(t)}{dt} = 4k_1B_1(t)A_2(t) + 2k_2B_1(t)A_4(t) - 2k_1A^1(t)A_6(t) - 2k_2A^2(t)A_6(t) - 2k_1B_1(t)A_6(t) - k_1B_2(t)A_6(t) - 2k_1C_jA_6(t) \quad (22)$$

$$\frac{dA_7(t)}{dt} = 2k_1B_2(t)A_2(t) + 2k_2B_1(t)A_5(t) + k_1A^1(t)A_6(t) + k_2A^2(t)A_6(t) - k_1A^1(t)A_7(t) - k_2A^2(t)A_7(t) - 2k_1B_1(t)A_7(t) - k_1B_2(t)A_7(t) - k_1C_jA_7(t) \quad (23)$$

$$\frac{dA_8(t)}{dt} = 4k_1B_1(t)A_3(t) + k_2B_2(t)A_4(t) + k_1A^1(t)A_6(t) + k_2A^2(t)A_6(t) - k_1A^1(t)A_8(t) - k_2A^2(t)A_8(t) - 2k_1B_1(t)A_8(t) - k_1B_2(t)A_8(t) - k_1C_jA_8(t) \quad (24)$$

$$\frac{dA_9(t)}{dt} = 2k_1B_2(t)A_3(t) + k_2B_2(t)A_5(t) + k_1A^1(t)A_7(t) + k_2A^2(t)A_7(t) + k_1A^1(t)A_8(t) + k_2A^2(t)A_8(t) - k_1B_2(t)A_9(t) - 2k_1B_1(t)A_9(t) \quad (25)$$

$$\frac{dA_{10}(t)}{dt} = 2k_1B_1(t)A_4(t) - 2k_1A^1(t)A_{10}(t) - 2k_2A^2(t)A_{10}(t) - 2k_2B_1(t)A_{10}(t) - k_2B_2(t)A_{10}(t) - 2k_2C_jA_{10}(t) \quad (26)$$

$$\frac{dA_{11}(t)}{dt} = k_1B_2(t)A_4(t) + 2k_1B_1(t)A_5(t) + 2k_1A^1(t)A_{10}(t) + 2k_2A^2(t)A_{10}(t) - k_1A^1(t)A_{11}(t) - k_2A^2(t)A_{11}(t) - 2k_2B_1(t)A_{11}(t) - k_2B_2(t)A_{11}(t) - k_2C_jA_{11}(t) \quad (27)$$

$$\frac{dA_{12}(t)}{dt} = k_1B_2(t)A_5(t) + k_1A^1(t)A_{11}(t) + k_2A^2(t)A_{11}(t) - 2k_2B_1(t)A_{12}(t) - k_2B_2(t)A_{12}(t) \quad (28)$$

$$\frac{dA_{13}(t)}{dt} = 2k_1B_1(t)A_6(t) + 2k_2B_1(t)A_{10}(t) - 3k_1A^1(t)A_{13}(t) - 3k_2A^2(t)A_{13}(t) \quad (29)$$

$$\frac{dA_{14}(t)}{dt} = k_1B_2(t)A_6(t) + 2k_1B_1(t)A_7(t) + 2k_2B_1(t)A_{11}(t) + 2k_1A^1(t)A_{13}(t) + 2k_2A^2(t)A_{13}(t) - 2k_1A^1(t)A_{14}(t) - 2k_2A^2(t)A_{14}(t) \quad (30)$$

$$\frac{dA_{15}(t)}{dt} = k_1B_2(t)A_7(t) + 2k_2B_1(t)A_{12}(t) + k_1A^1(t)A_{14}(t) + k_2A^2(t)A_{14}(t) - k_1A^1(t)A_{15}(t) - k_2A^2(t)A_{15}(t) \quad (31)$$

$$\frac{dA_{16}(t)}{dt} = k_1B_2(t)\,A_9(t) + k_2B_2(t)A_{12}(t) + k_1A^1(t)A_{15}(t) + k_2A^2(t)A_{15}(t) + k_1A^1(t)A_{18}(t) + k_2A^2(t)A_{18}(t) \quad (32)$$

$$\frac{dA_{17}(t)}{dt} = 2k_1B_1(t)A_8(t) + k_2B_2(t)A_{10}(t) + k_1A^1(t)A_{13}(t) + k_2A^2(t)A_{13}(t) - 2k_1A^1(t)A_{17}(t) - 2k_2A^2(t)A_{17}(t) \quad (33)$$

$$\frac{dA_{18}(t)}{dt} = k_1B_2(t)A_8(t) + 2k_1B_1(t)A_9(t) + k_2B_2(t)A_{11}(t) + k_1A^1(t)A_{14}(t) + k_2A^2(t)A_{14}(t) + 2k_1A^1(t)A_{17}(t) + 2k_2A^2(t)A_{17}(t) - k_1A^1(t)A_{18}(t) - k_2A^2(t)A_{18}(t) \quad (34)$$

$$\frac{dA_{19}(t)}{dt} = k_1C_jA_6(t) + 2k_2C_jA_{10}(t) - k_1A^1(t)A_{19}(t) - k_2A^2(t)A_{19}(t) + 2k_1B_1(t)A_{21}(t) \quad (35)$$

$$\frac{dA_{20}(t)}{dt} = k_1C_jA_7(t) + k_2C_jA_{11}(t) + k_1A^1(t)A_{19}(t) + k_2A^2(t)A_{19}(t) + k_1B_2(t)A_{21}(t) \quad (36)$$

$$\frac{dA_{21}(t)}{dt} = 2k_1C_jA_2(t) + k_2C_jA_4(t) - 2k_1B_1(t)A_{21}(t) - k_1B_2(t)A_{21}(t) \quad (37)$$

$$\frac{dA_{22}(t)}{dt} = k_1C_jA_6(t) - k_1A^1(t)A_{22}(t) - k_2A^2(t)A_{22}(t) + 2k_2B_1(t)A_{24}(t) \quad (38)$$

$$\frac{dA_{23}(t)}{dt} = k_1C_jA_8(t) + k_1A^1(t)A_{22}(t) + k_2A^2(t)A_{22}(t) + k_2B_2(t)A_{24}(t) \quad (39)$$

$$\frac{dA_{24}(t)}{dt} = k_1C_jA_4(t) - 2k_2B_1(t)A_{24}(t) - k_2B_2(t)A_{24}(t) \quad (40)$$

In the above equations, the following concentration definitions (eqs 41−46) are used:

$$B_1(t) = B_1(0) - B_2(t) - B_3(t) - B_4(t) \quad (41)$$

$$B_2(t) = A_2(t) + A_4(t) + 2A_6(t) + A_7(t) + A_8(t) + 2A_{10}(t) + A_{11}(t) + 3A_{13}(t) + 2A_{14}(t) + A_{15}(t) + 2A_{17}(t) + A_{18}(t) + A_{19}(t) + A_{22}(t) \quad (42)$$

$$B_3(t) + \frac{1}{2}\{A_3(t) + A_5(t) + A_7(t) + A_8(t) + 2A_9(t) + A_{11}(t) + 2A_{12}(t) + A_{14}(t) + 2A_{15}(t) + 3A_{16}(t) + A_{17}(t) + 2A_{18}(t) + A_{20}(t) + A_{23}\} \quad (43)$$

$$B_4(t) = A_{19}(t) + A_{20}(t) + A_{21}(t) + A_{22}(t) + A_{23}(t) + A_{24}(t) \quad (44)$$

$$A^1(t) = 2A_1(t) + 2A_2(t) + 2A_3(t) + A_4(t) + A_5(t) + A_6(t) + A_7(t) + A_8(t) + A_9(t) + A_{21}(t) \quad (45)$$

$$A^2(t) = A_1(t) + A_4(t) + A_5(t) + A_{10}(t) + A_{11}(t) + A_{12}(t) + A_{24}(t) \quad (46)$$

The expression for C_j was given in the text (eq 3).

Equations 17−46 are solved numerically using Gear's method, with the initial condition given in eq 47.

$$A_1(0) = [\text{A monomer}]_0; \quad A_i(0) = 0 \quad \forall i \neq 1$$
$$B_1(0) = [\text{B monomer}]_0; \quad B_i(0) = 0 \quad \forall i \neq 1 \quad (47)$$

Calculation of the Expected Weight Given That an A or B Monomer Is Selected, Respectively. The expected weight given an A monomer is selected ($E(W|\text{A root})$) and the expected weight given a B monomer is selected ($E(W|\text{B root})$) are calculated as follows. Once a root is chosen, the probability that this root is a particular structure of those defined in Figure 1 is calculated as a number fraction, as indicated in eqs 48 and 49.

$$P(A_i|\text{A root}) = \frac{A_i(t)}{A_1(0)} \quad (48)$$

$$P(B_i|\text{B root}) = \frac{B_i(t)}{B_1(0)} \quad (49)$$

Now, in the case where an A root was chosen, the expected weight is

$$E(W|\text{A root}) = \sum_{i=1}^{24} E(W|A_i)\frac{A_i(t)}{A_1(0)} \quad (50)$$

This leads to the problem of calculating the expected weight given an A_i root was chosen, $E(W|A_i)$. For example, the expected weights associated with A_2 and A_{11} are

$$E(W|A_2) = M_A + M_B \quad (51)$$

$$E(W|A_{11}) = M_A + 2M_B + E(W^{out}B_3) \quad (52)$$

where $E(W^{out}B_3)$ is the expected weight "looking out"

from B_3. The evaluation of this quantity is shown later in the paper. The remaining terms are obtained similarly. Finally, when the appropriate terms are substituted into eq 50, eq 53 results.

$$E(W|\text{A root}) = M_A + \frac{1}{A_1(0)}(M_B(B_2(t) + 2B_3(t) + B_4(t)) + 2B_3(t)E(W^{out}B_3)) \quad (53)$$

The expected weight looking out from B_3, $E(W^{out}B_3)$, is calculated, making again use of a conditional expectation, as given by eq 54.

$$E(W^{out}B_3) = M_A + \frac{1}{2}\sum_{i=1}^{24} E(W^{out}A_i \text{ from } B_3)\, P(A_i|B_3) \quad (54)$$

The conditional expectations in eq 54 are calculated as

$$E(W^{out}A_i \text{ from } B_3) = M_B \quad i = 7, 8, 11, 20, 23 \quad (55)$$

$$E(W^{out}A_i \text{ from } B_3) = M_B + E(W^{out}B_3) \quad i = 9, 12 \quad (56)$$

$$E(W^{out}A_i \text{ from } B_3) = 2M_B \quad i = 14, 17 \quad (57)$$

$$E(W^{out}A_i \text{ from } B_3) = 2M_B + E(W^{out}B_3) \quad i = 15, 18 \quad (58)$$

$$E(W^{out}A_i \text{ from } B_3) = 2M_B + 2E(W^{out}B_3) \quad i = 16 \quad (59)$$

and the conditional probabilities are evaluated as

$$P(A_i|B_3) = \frac{A_i(t)}{B_3(t)} \quad i = 7, 8, 11, 14, 17, 20, 23 \quad (60)$$

$$P(A_i|B_3) = \frac{2A_i(t)}{B_3(t)} \quad i = 9, 12, 15, 18 \quad (61)$$

$$P(A_i|B_3) = \frac{3A_i(t)}{B_3(t)} \quad i = 16 \quad (62)$$

$$P(A_i|B_3) = 0 \quad \text{for the remaining values of } i \quad (63)$$

Some extra algebraic effort is needed to obtain $E(W^{out}B_3)$ since it appears on both sides of eq 54. Finally, eq 64 results:

$$E(W^{out}B_3) = \{M_A\, 2B_3(t) + M_B[A_7(t) + A_8(t) + 2A_9(t) + A_{11}(t) + 2A_{12}(t) + 2A_{14}(t) + 4A_{15}(t) + 6A_{16}(t) + 2A_{17}(t) + 4A_{18}(t) + A_{20}(t) + A_{23}(t)]\}/\{2 \times B_3(t) - 2A_9(t) - 2A_{12}(t) - 2A_{15}(t) - 6A_{16}(t) - 2A_{18}(t)\} \quad (64)$$

Similarly, the expected weight when a B root is selected is given by the following equations:

$$E(W|B \text{ root}) = \sum_{i=1}^{24} E(W|B_i)\frac{B_i(t)}{B_1(0)} \quad (65)$$

with

$$E(W|B_1) = M_B \quad (66)$$

$$E(W|B_2) = M_A + M_B + \sum_{i=1}^{24} E(W^{out}A_i \text{ from } B_2)\, P(A_i|B_2) \quad (67)$$

$$E(W|B_3) = M_B + 2E(W^{out}B_3) \quad (68)$$

$$E(W|B_4) = M_A + M_B + \sum_{i=1}^{24} E(W^{out}A_i \text{ from } B_4)\, P(A_i|B_4) \quad (69)$$

For the evaluation of $E(W|B_2)$ we need to consider the conditional expectations calculated as

$$E(W^{out}A_i \text{ from } B_2) = M_B \quad i = 6, 10, 19, 22 \quad (70)$$

$$E(W^{out}A_i \text{ from } B_2) = M_B + E(W^{out}B_3) \quad i = 7, 8, 11 \quad (71)$$

$$E(W^{out}A_i \text{ from } B_2) = 2M_B \quad i = 13 \quad (72)$$

$$E(W^{out}A_i \text{ from } B_2) = 2M_B + E(W^{out}B_3) \quad i = 14, 17 \quad (73)$$

$$E(W^{out}A_i \text{ from } B_2) = 2M_B + 2E(W^{out}B_3) \quad i = 15, 18 \quad (74)$$

$$E(W^{out}A_i \text{ from } B_2) = 0 \quad \text{for the remaining values of } i \quad (75)$$

and the conditional probabilities as

$$P(A_i|B_2) = \frac{2A_i(t)}{B_2(t)} \quad i = 6, 10, 14, 17 \quad (76)$$

$$P(A_i|B_2) = \frac{A_i(t)}{B_2(t)} \quad i = 2, 4, 7, 8, 11, 15, 18, 19, 22 \quad (77)$$

$$P(A_{13}|B_2) = \frac{3A_{13}(t)}{B_2(t)} \quad (78)$$

$$P(A_i|B_2) = 0 \quad \text{for the remaining values of } i \quad (79)$$

Similarly, for the evaluation of $E(W|B_4)$ the conditional expectations must be calculated as

$$E(W^{out}A_i \text{ from } B_4) = M_B \quad i = 19, 22 \quad (80)$$

$$E(W^{out}A_i \text{ from } B_4) = M_B + E(W^{out}B_3) \quad i = 20, 23 \quad (81)$$

$$E(W^{out}A_i \text{ from } B_4) = 0 \quad \text{for the remaining values of } i \quad (82)$$

and the conditional expectations as

$$P(A_i|B_4) = \frac{A_i(t)}{B_4(t)} \quad i = 19, ..., 24 \quad (83)$$

$$P(A_i|B_4) = 0 \quad \text{for the remaining values of } i \quad (84)$$

The final result for the expected weight given that a B root is chosen is obtained by substituting eqs 66−84 into eq 65.

Calculation of the Probabilities of Having Chosen a Finite Molecule Given That the Root Was Either an A or B Monomer, Respectively. We calculate these quantities, $P(F|\text{A root})$ and $P(F|\text{B root})$, by conditioning on the probabilities of finding finite ends given that a particular A_i or B_i was selected, as follows:

$$P(F|\text{A root}) = \sum_{i=1}^{24} P(F|A_i)P(A_i|\text{A root}) = \sum_{i=1}^{24} P(F|A_i)\frac{A_i}{A_1(0)} \quad (85)$$

$$P(F|\text{B root}) = \sum_{i=1}^{4} P(F|B_i)P(B_i|\text{B root}) = \sum_{i=1}^{4} P(F|B_i)\frac{B_i}{B_1(0)} \quad (86)$$

Each of the $P(F|A_i)$ values is found by inspection. For example, if we indicate as $P(F^{\text{out}}B_3)$ the probability of finding that the molecule is finite when looking out of a B_3 unit we would get

$$P(F|A_1) = 1 \quad (87)$$

$$P(F|A_{11}) = P(F^{\text{out}}B_3) \quad (88)$$

$$P(F|A_{15}) = P(F^{\text{out}}B_3)^2 \quad (89)$$

The remaining conditional probabilities are found in a similar way. Replacing them into eq 85 we find

$$A_1(0)P(F|\text{A root}) = A_1(t) + A_2(t) + A_4(t) + A_6(t) + A_{10}(t) + A_{13}(t) + A_{19}(t) + A_{21}(t) + A_{22}(t) + A_{24}(t) + P(F^{\text{out}}B_3) \times \left(A_3(t) + A_5(t) + A_7(t) + A_8(t) + A_{11}(t) + A_{14}(t) + A_{17}(t) + A_{20}(t) + A_{23}(t)\right) + P(F^{\text{out}}B_3)^2(A_9(t) + A_{12}(t) + A_{15}(t) + A_{18}(t)) + P(F^{\text{out}}B_3)^3 A_{16}(t) \quad (90)$$

In turn, the conditional probabilities of finding finite ends given a particular B structure was chosen as a root are found by conditioning as

$$P(F|B_1) = 1 \quad (91)$$

$$P(F|B_i) = \sum_{j=1}^{24} P(F^{\text{in}}\ A_j \text{ from } B_i)P(A_j|B_i) \quad i = 2, 4 \quad (92)$$

$$P(F|B_3) = \left(\sum_{j=1}^{24} P(F^{\text{in}}\ A_j \text{ from } B_3)P(A_j|B_3)\right)^2 = (P(F^{\text{out}}B_3))^2 \quad (93)$$

Here $P(F^{\text{in}}\ A_j \text{ from } B_i)$ is the probability of finding that the molecule is finite when looking into an A_j structure. For example

$$P(F^{\text{in}}\ A_6 \text{ from } B_2) = 1 \quad (94)$$

$$P(F^{\text{in}}\ A_{11} \text{ from } B_2) = P(F^{\text{out}}B_3) \quad (95)$$

$$P(F^{\text{in}}\ A_{11} \text{ from } B_3) = 1 \quad (96)$$

$$P(F^{\text{in}}\ A_{16} \text{ from } B_3) = P(F^{\text{out}}B_3)^2 \quad (97)$$

The remaining conditional probabilities are found in a similar way. The final result for B roots is

$$B_1(0)P(F|\text{B root}) = B_1(t) + A_2(t) + A_4(t) + 2A_6(t) + 2A_{10}(t) + 3A_{13}(t) + 2A_{19}(t) + A_{21}(t) + 2A_{22}(t) + A_{24}(t) + P(F^{\text{out}}B_3)(A_7(t) + A_8(t) + A_{11}(t) + 2A_{14}(t) + 2A_{17}(t) + A_{20}(t) + A_{23}(t)) + P(F^{\text{out}}B_3)^2(A_{15}(t) + A_{18}(t) + B_3(t)) \quad (98)$$

To find $P(F^{\text{out}}B_3)$, one must solve eq 93. The following quadratic expression results after substitution of the appropriate terms.

$$3A_{16}(t)(P(F^{\text{out}}B_3))^2 + 2(A_9(t) + A_{12}(t) + A_{15}(t) + A_{18}(t) - B_3(t))P(F^{\text{out}}B_3) + A_3(t) + A_5(t) + A_7(t) + A_8(t) + A_{11}(t) + A_{14}(t) + A_{17}(t) + A_{20}(t) + A_{23}(t) = 0 \quad (99)$$

This expression must be solved for the root that lies between zero and one. Substituting the result into the above equations makes it possible to find the values of the probabilities $P(F|\text{A root})$ and $P(F|\text{B root})$. In turn, substitution of the latter into eq 9 allows the calculation of the sol fraction w_s as a function of time.

Calculation of the Probabilities That a Structure Is Part of the Elastically Effective Material Given That Either an A Monomer or a B Monomer Was Selected. These quantities, $P(\text{el.eff}|\text{A root})$ and $P(\text{el.eff}|\text{B root})$, are calculated according to eqs 100 and 101.

$$A_1(0)P(\text{el.eff}|\text{A root}) = (1 - P(F^{\text{out}}B_3))^2 (A_9(t) + A_{12}(t) + A_{15}(t) + A_{18}(t)) + (1 - P(F^{\text{out}}B_3))^3 A_{16}(t) + 3P(F^{\text{out}}B_3)(1 - P(F^{\text{out}}B_3))^2 A_{16}(t) \quad (100)$$

$$B_1(0)P(\text{el.eff}|\text{B root}) = (1 - P(F^{\text{out}}B_3))^2 B_3(t) \quad (101)$$

References and Notes

(1) Flory, P. J. *Principles of Polymer Chemistry*, Cornell University Press: Ithaca, NY, 1953, Chapter IX.
(2) Stockmayer, W. H. *J. Polym. Sci.* **1952**, *9*, 69−71.
(3) Stockmayer, W. H. *J. Polym. Sci.* **1953**, *11*, 424.
(4) Gordon, M. *Proc. R. Soc. London, Ser A* **1962**, *268*, 240−259.
(5) Stanford, J. L.; Stepto, R. F. T. *J. Chem. Soc., Faraday Trans. 1* **1975**, 1292−2007.
(6) Macosko, C. W.; Miller, D. R. *Macromolecules* **1976**, *9*, 199−206.
(7) Miller, D. R.; Macosko, C. W. *Macromolecules* **1978**, *11*, 656−662.
(8) Gordon, M.; Scantlebury, G. R. *Trans. Faraday Soc.* **1964**, *60*, 604−621.
(9) Mikeš, J.; Dušek, K. *Macromolecules* **1982**, *15*, 93−99.
(10) Galina, H.; Szustalewicz, A. *Macromolecules* **1989**, *22*, 3124−3129.
(11) Miller, D. R.; Macosko, C. W. *Macromolecules* **1980**, *13*, 1063−1069.

(12) Sarmoria, C.; Miller, D. R. *Macromolecules* **1991**, *24*, 1833−1845.
(13) Martinelli, F. J. *J. Polym. Sci., Polym. Phys.* **1978**, *16*, 1519−1527.
(14) Dušek, K.; Ilavský, M.; Lunák, S. *J. Polym. Sci., Symp.* **1975**, *53*, 29−44.
(15) Gordon, M.; Temple, W. B. *Makromol. Chem.* **1972**, *160*, 263−276.
(16) Temple, W. B. *Makromol. Chem.* **1972**, *160*, 277−289.
(17) Leung, Y.; Eichinger, B. E. *J. Chem. Phys.* **1984**, *80*, 3877−3884.
(18) Leung, Y.; Eichinger, B. E. *J. Chem. Phys.* **1984**, *80*, 3885−3891.
(19) Dutton, S.; Stepto, R. F. T.; Taylor, D. J. R. *Angew. Makromol. Chem.* **1996**, *240*, 39−57.
(20) Rolfes, H.; Stepto, R. F. T. *Polym. Gels Networks* **1994**, *2*, 149−157.
(21) Dušek, K.; Gordon, M.; Ross-Murphy S. B. *Macromolecules* **1978**, *11*, 236−245.
(22) Ilavský, M.; Dušek, K. *Macromolecules* **1986**, *19*, 2139−2146.
(23) Stanford, J. L.; Stepto, R. F. T.; Waywell, D. R. *J. Chem. Soc., Faraday Trans. 1* **1975**, *71*, 1308−1326.
(24) Rolfes, H.; Stepto, R. F. T. *Makromol. Chem., Macromol. Symp.* **1990**, *40*, 61−79.
(25) Rolfes, H.; Stepto, R. F. T. *Makromol. Chem., Macromol. Symp.* **1993**, *65*, 233−242.
(26) Sarmoria, C.; Vallés, E.; Miller, D. *Makromol. Chem., Macromol. Symp.* **1986**, *2*, 69−87.
(27) Sarmoria, C.; Vallés, E. M.; Miller, D. R. *Macromolecules* **1990**, *23*, 580−589.
(28) Miller, D. R.; Macosko, C. W. In *Biological and Synthetic Polymer Networks*; Kramer, O., Ed.; Elsevier Applied Science, New York, 1986; pp 219−242.
(29) Au-chin, T.; Ze-sheng, L.; Chia-chung, S.; Xin-yi, T. *Macromolecules* **1988**, *21*, 797−804.
(30) Rolfes, H.; Stepto, R. F. T. *Makromol. Chem., Macromol. Symp.* **1993**, *76*, 1−12.
(31) Dutton, S.; Rolfes, H.; Stepto, R. F. T. *Polymer* **1994**, *35*, 4521−4526.
(32) Sarmoria, C.; Miller, D. R. *Comput. Theor. Polym. Sci.* **2001**, *11*, 113−127.
(33) Dobson, G. R.; Gordon, M. *J. Chem. Phys.* **1964**, *41*, 2389−2398.
(34) Gordon, M.; Scantlebury, G. R. *J. Chem. Soc. B* **1967**, 1−13.
(35) Kasehagen, L. J.; Rankin, S. E.; McCormick, A. V.; Macosko, C. W. *Macromolecules* **1997**, *30*, 3921−3929.
(36) Fahey, D. R.; Hensley, H. D.; Ash, C. E.; Senn, D. R. *Macromolecules* **1997**, *30*, 387−393.
(37) Lee, K. J.; Eichinger, B. E. *Polymer* **1990**, *31*, 406−413.
(38) Stockmayer, W. H. In *Advancing Fronts in Chemistry*; Twiss, S. B., Ed.; Reinhold Publishing Corp.: New York, 1945; Vol. I.
(39) Flory, P. J. *Principles of Polymer Chemistry*, Cornell University Press: Ithaca, NY, 1953; p 354.
(40) Kilb, R. W. *J. Phys. Chem.* **1958**, *62*, 969−971.
(41) Price, F. P.; Gibbs, J. H.; Zimm, B. H. *J. Phys. Chem.* **1958**, *62*, 972−976.
(42) Price, F. P. *J. Phys. Chem.* **1958**, *62*, 977−978.
(43) Mark, J. E.; Curro, J. G. *J. Chem. Phys.* **1983**, *79*, 5705−5709.
(44) Flory, P. J. *Principles of Polymer Chemistry*; Cornell University Press: Ithaca, NY, 1953, Chapter X.
(45) Ross, S. M. *Introduction to Probability Models*; Academic Press: San Diego, CA, 1993.
(46) Kienle, R. H.; van der Meulen, P. A.; Petke, F. E. *J. Am. Chem. Soc.* **1939**, *61*, 2268−2271.
(47) Kienle, R. H.; Petke, F. E. *J. Am. Chem. Soc.* **1940**, *62*, 1053−1056.
(48) Kienle, R. H.; Petke, F. E. *J. Am. Chem. Soc.* **1941**, *63*, 481−484.
(49) Belgacem, M. N.; Quillerou, J.; Gandini, A.; Rivero, J.; Roux, G. *Eur. Polym. J.* **1989**, *25*, 1125−1130.

MA001438M